Natural Resources for Human Health

eISSN: 2583-1194

Original Research

Received 28 July 2026
Revised 29 August 2026
Accepted 12 September 2026

Natural Resources for Human Health 2026, Vol. 6 (9s): 1175–1188

KEYWORDS:
Nephroprotection, Cisplatin toxicity, HEK-293 cells, Oxidative stress, Polyherbal extract, Apoptosis

Protective Effects of a Polyherbal Combination of *Ajuga Bracteosa* and *Gynura procumbens* on Cisplatin-Induced Renal Cytotoxicity Through Modulation of ROS-Mediated Apoptotic Pathways in HEK-293 Cells

Beema Jainab S.I[1], K.V. Parthasarathi[2], Sujatha Samala[3*], Paresh Ashok Patil[4], Rajni Yadav[5], Tej Pratap Singh[6], Prasenjit Mishra[7], Ketan Girish Bhutkar[8],

[1]Department of Botany, Justice Basheer Ahmed Sayeed College for Women (Autonomous), Chennai -600 018. Tamil Nadu, India.
[2]Department of Pharmaceutical Chemistry & Analysis, KS Rangasamy College of Pharmacy
Thiruchencode - 637 215 The Tamil Nadu Dr. MGR Medical University Chennai.
[3]Department of Pharmacognosy and Phytochemistry, University College of Pharmaceutical Sciences, Palamuru University, Mahabubnagar-509001, Telangana.
[4]Ahinsa Institute of Pharmacy, Dondaicha. Dhule Road, Dondaicha, Tal-shindkheda,Dist- Dhule State-Maharastra (425408).
[5]Kalinga University, Faculty of Pharmacy, Naya Raipur,492101 Chhattisgarh.
[6]Department of Pharmaceutics, Satyadeo College of Pharmacy, Borsiya, Fadanpur, Ghazipur Uttar Pradesh Pin code: 233001.
[7]Department of Pharmacology, Einstein college of Pharmacy, Baniatangi, Khordha, Odisha Pin: 752060.
[8]Department of Pharmacognosy, Trinity college of Pharmacy Pune, Pin-411048.
Corresponding Author**
Sujatha Samala*
[3]Department of Pharmacognosy and Phytochemistry, University College of Pharmaceutical Sciences, Palamuru University, Mahabubnagar-509001, Telangana.
Email id: - sujathasamala@gmail.com

ABSTRACT: Cisplatin-induced nephrotoxicity remains a major limitation in chemotherapy, primarily mediated through oxidative stress and apoptosis in renal cells. The present study evaluated the nephroprotective potential of a hydroalcoholic polyherbal extract comprising Ajuga bracteosa and Gynura procumbens (1:1) against cisplatin-induced cytotoxicity in HEK-293 cells. Cytotoxicity was induced using cisplatin (20 µM), while the extract was tested at 25, 50, and 100 µg/mL concentrations following pre-treatment. Cell viability was assessed using the MTT assay, and membrane integrity was evaluated by lactate dehydrogenase (LDH) release. Oxidative stress parameters were analyzed through intracellular reactive oxygen species (ROS) generation, lipid peroxidation (MDA levels), and endogenous antioxidant enzymes (SOD, CAT, and GSH). Mitochondrial membrane potential (ΔΨm) was determined using JC-1 dye, while apoptosis was assessed via caspase-3 activity. Cisplatin exposure significantly reduced cell viability, increased ROS production, induced lipid peroxidation, disrupted mitochondrial function, and elevated caspase-3 activity. Pre-treatment with the polyherbal extract demonstrated a dose-dependent protective effect, restoring cell viability, reducing

oxidative stress, preserving mitochondrial integrity, and suppressing apoptosis. The highest extract concentration (100 µg/mL) exhibited effects comparable to the standard antioxidant N-acetylcysteine. The findings suggest that the polyherbal extract confers nephroprotection through modulation of the oxidative stress–mitochondrial apoptosis axis, indicating its potential as a supportive therapeutic strategy against cisplatin-induced renal toxicity.

1. INTRODUCTION

Cisplatin is a platinum-based chemotherapeutic agent widely used in the treatment of various solid tumors, including lung, ovarian, testicular, and bladder cancers. Despite its proven clinical efficacy, its therapeutic application is significantly limited by dose-dependent nephrotoxicity, which remains one of the most critical adverse effects associated with its use. The kidneys, particularly the proximal tubular epithelial cells, are highly susceptible to cisplatin-induced damage due to preferential drug accumulation and activation of multiple pathological pathways. Consequently, nephrotoxicity not only compromises renal function but also necessitates dose reduction or discontinuation of therapy, ultimately affecting treatment outcomes (Umar et al., 2021; Wang et al., 2023; Wróblewska et al., 2024; Wróblewska et al., 2022).

The pathogenesis of cisplatin-induced nephrotoxicity is complex and multifactorial, involving oxidative stress, inflammation, mitochondrial dysfunction, and apoptosis. Among these, oxidative stress plays a central role, characterized by excessive generation of reactive oxygen species (ROS) that overwhelm the endogenous antioxidant defence system. This imbalance leads to lipid peroxidation, protein oxidation, DNA damage, and disruption of cellular homeostasis. Furthermore, ROS-mediated damage directly impacts mitochondrial integrity, resulting in loss of mitochondrial membrane potential, release of pro-apoptotic factors, and activation of intrinsic apoptotic pathways, including caspase-3 signalling. Therefore, targeting oxidative stress and its downstream consequences represents a rational therapeutic strategy for mitigating cisplatin-induced renal injury (Farouk et al., 2025; Gazwi et al., 2024; L. Li et al., 2024). In recent years, increasing attention has been directed toward the use of plant-based therapeutics due to their rich phytochemical composition and multi-targeted pharmacological effects. Herbal extracts are known to contain bioactive constituents such as flavonoids, phenolic compounds, alkaloids, and terpenoids, which exhibit potent antioxidant and cytoprotective properties. Unlike synthetic agents that often act on a single pathway, herbal formulations offer synergistic effects by modulating multiple cellular mechanisms simultaneously, making them particularly suitable for complex pathological conditions such as drug-induced nephrotoxicity (Davoudi et al., 2022; Gazwi et al., 2024).

Ajuga bracteosa, a medicinal plant belonging to the Lamiaceae family, has been traditionally used for its anti-inflammatory, antioxidant, and hepatoprotective properties. Phytochemical investigations have revealed the presence of flavonoids, phenolics, and iridoid glycosides, which contribute to its free radical scavenging activity. Similarly, *Gynura procumbens*, commonly known as "longevity spinach," has gained recognition for its diverse pharmacological activities, including antioxidant, anti-inflammatory, and cytoprotective effects. The plant is rich in polyphenols and flavonoids, which have been shown to modulate oxidative stress pathways and enhance cellular defence mechanisms (Nazer et al., 2022; Raja et al., 2023; Tithi et al., 2023).

The rationale for combining *Ajuga bracteosa* and *Gynura procumbens* lies in the potential for synergistic interaction between their bioactive constituents. A polyherbal approach may provide enhanced efficacy compared to individual extracts by targeting multiple aspects of cisplatin-induced cellular injury, particularly oxidative stress and apoptosis. However, despite the promising pharmacological profiles of these plants, their combined nephroprotective potential against cisplatin-induced toxicity has not been extensively investigated, especially at the cellular and mechanistic levels. Human embryonic kidney (HEK-293) cells serve as a well-established in vitro model for studying renal cytotoxicity and protective interventions. These cells provide a controlled environment to evaluate cellular responses, including oxidative stress, mitochondrial dysfunction, and apoptosis, enabling mechanistic insights into nephroprotective effects (Nazer et al., 2022; Raja et al., 2023; Tithi et al., 2023).

Therefore, the present study was designed to evaluate the nephroprotective activity of a hydroalcoholic polyherbal extract of *Ajuga bracteosa* and *Gynura procumbens* (1:1) against cisplatin-induced toxicity in HEK-293 cells. The study specifically aimed to investigate the role of the extract in modulating oxidative stress, preserving mitochondrial function, and inhibiting apoptosis, thereby establishing its potential as a supportive therapeutic strategy in reducing chemotherapy-induced renal damage.

3. MATERIALS AND METHODS

3.1 Materials

Cisplatin (purity ≥99%) was procured from Sigma-Aldrich. Dulbecco's Modified Eagle Medium (DMEM), fetal bovine serum (FBS), penicillin-streptomycin solution, trypsin-EDTA, and phosphate-buffered saline (PBS) were obtained from Gibco. 3-(4,5-dimethylthiazol-2-yl)-2,5-diphenyl tetrazolium bromide (MTT), dichlorofluorescein diacetate (DCFH-DA), JC-1 dye, thiobarbituric acid (TBA), reduced glutathione (GSH), and assay kits for superoxide dismutase (SOD), catalase (CAT), and caspase-3 were purchased from HiMedia Laboratories.

All other reagents and solvents used in the study were of analytical grade and used without further purification.

3.2 Plant Material and Extraction

Fresh aerial parts of *Ajuga bracteosa* were collected from a verified natural habitat and authenticated by a qualified taxonomist. The plant material was washed, shade-dried at room temperature, and pulverized into a coarse powder using a mechanical grinder. Approximately 250 g of powdered material was subjected to Soxhlet extraction using methanol for 24 hours. The extract was filtered and concentrated under reduced pressure using a rotary evaporator. The obtained semisolid mass was further dried in a desiccator and stored at 4°C until further use. The percentage yield of the extract was calculated, and the extract was reconstituted in dimethyl sulfoxide (DMSO) to prepare stock solutions.

3.3 Phytochemical Standardization

The methanolic extract was subjected to preliminary phytochemical screening for alkaloids, flavonoids, phenolics, saponins, and terpenoids using standard qualitative methods. Total phenolic content was estimated using the Folin–Ciocalteu method and expressed as mg gallic acid equivalents (GAE)/g extract. Total flavonoid content was determined using the aluminium chloride method and expressed as mg quercetin equivalents (QE)/g extract.

3.4 Cell Line and Culture Conditions

Human embryonic kidney cells (HEK-293) were obtained from National Centre for Cell Science, Pune, India. Cells were cultured in DMEM supplemented with 10% FBS and 1% penicillin-streptomycin. The cells were maintained at 37°C in a humidified incubator with 5% CO_2 atmosphere. Cells were subcultured upon reaching 70–80% confluency using trypsin-EDTA and used for experiments between passages 5 and 20.

3.5 Experimental Design

The study was designed to evaluate the nephroprotective effect of the extract against cisplatin-induced cytotoxicity. Cells were divided into the following groups:

- Control group (untreated cells)
- Cisplatin-treated group (toxic control)
- Extract-treated groups (25, 50, 100 µg/mL)
- Cisplatin + extract groups (pre-treatment model)
- Cisplatin + N-acetylcysteine group (positive control)

Cells in treatment groups were pre-treated with the extract for 24 hours followed by exposure to cisplatin for an additional 24 hours.

3.6 Determination of Cytotoxicity (MTT Assay)

Cell viability was assessed using the MTT assay. HEK-293 cells were seeded in 96-well plates at a density of 1×10^4 cells per well and allowed to attach overnight. After treatment, 20 µL of MTT solution (5 mg/mL) was added to each well and incubated for 4 hours. The formed formazan crystals were dissolved in DMSO, and absorbance was measured at 570 nm using a microplate reader. Cell viability (%) was calculated relative to control cells (Zakeri-Milani et al., 2021; M. Zheng et al., 2025; Zohmachhuana et al., 2022).

3.7 Determination of Cisplatin IC_{50}

To establish an optimal nephrotoxic concentration, HEK-293 cells were exposed to increasing concentrations of cisplatin (5, 10, 20, 30, and 40 µM) for 24 hours. Cell viability was determined using the MTT assay as described previously. The IC_{50} value was calculated from the dose–response curve using nonlinear regression analysis. Based on preliminary observations, a concentration inducing approximately 50–60% reduction in cell viability (~20 µM) was selected as the working toxic dose for subsequent experiments (Zakeri-Milani et al., 2021; M. Zheng et al., 2025; Zohmachhuana et al., 2022).

3.8 Determination of Safe Concentration Range of Extract

The hydroalcoholic extract of *Ajuga bracteosa* and *Gynura procumbens* (1:1) was evaluated for cytotoxicity in HEK-293 cells at concentrations ranging from 10 to 200 µg/mL. Cells were treated for 24 hours, and viability was assessed using the MTT assay. Concentrations showing ≥90% cell viability were considered non-toxic and selected for nephroprotective evaluation. Based on this criterion, 25, 50, and 100 µg/mL were fixed as low, medium, and high doses, respectively.

3.9 Lactate Dehydrogenase (LDH) Release Assay

Cell membrane integrity was assessed by measuring LDH release into the culture medium. After treatment, the culture supernatant was collected and analyzed using an LDH assay kit according to the manufacturer's protocol. Absorbance was measured at 490 nm, and LDH release (%) was calculated relative to the toxic control. Increased LDH levels indicated membrane damage, while reduction in LDH release in treated groups suggested cytoprotective effects (Sena-Torralba et al., 2025; Todorovic et al., 2021).

3.10 Intracellular Reactive Oxygen Species (ROS) Estimation

Intracellular ROS levels were quantified using the DCFH-DA fluorescent probe. After treatment, cells were incubated with 10 µM DCFH-DA for 30 minutes at 37°C. The fluorescence intensity was measured using a microplate reader at excitation/emission wavelengths of 485/530 nm. Results were expressed as percentage ROS generation relative to control. A decrease in fluorescence intensity in extract-treated groups indicated antioxidant activity (Zhang et al., 2023; Zhang et al., 2025).

3.11 Assessment of Mitochondrial Membrane Potential (ΔΨm)

Mitochondrial integrity was evaluated using JC-1 dye. After treatment, cells were incubated with JC-1 dye for 20 minutes at 37°C. Fluorescence was measured at dual wavelengths to determine the ratio of red (aggregates) to green (monomers) fluorescence. A decrease in red/green fluorescence ratio indicated mitochondrial depolarization, while restoration of this ratio in treated groups suggested mitochondrial protection (Su et al., 2024; Sun et al., 2024; Zhao et al., 2025; Zheng et al., 2022).

3.12 Lipid Peroxidation (MDA Estimation)

Lipid peroxidation was assessed by measuring malondialdehyde (MDA) levels using the thiobarbituric acid reactive substances (TBARS) assay. Cell lysates were mixed with TBA reagent and heated at 95°C for 30 minutes. After cooling, absorbance was measured at 532 nm.

MDA levels were expressed as nmol/mg protein. Increased MDA levels indicated oxidative damage, while reduction in treated groups reflected protective activity (R. Li et al., 2024; Phetruen et al., 2023; Saleh et al., 2021; Zou et al., 2024).

3.13 Estimation of Antioxidant Enzymes

Cell lysates were prepared and analyzed for endogenous antioxidant markers including superoxide dismutase (SOD), catalase (CAT), and reduced glutathione (GSH). SOD activity was determined based on inhibition of superoxide radicals. CAT activity was measured by monitoring decomposition of hydrogen peroxide. GSH levels were estimated using Ellman's reagent method. Results were expressed per mg protein and compared across groups (Lemus-de la Cruz et al., 2023; R. Li et al., 2024; Phetruen et al., 2023; Saleh et al., 2021; Zou et al., 2024).

3.14 Apoptosis Assessment (Caspase-3 Activity)

Caspase-3 activity was measured using a colorimetric assay kit. After treatment, cell lysates were incubated with a specific substrate, and the release of chromophore was measured at 405 nm. Increased caspase-3 activity indicated apoptosis induction, while reduction in treated groups confirmed anti-apoptotic effects of the extract (M. Y. Zheng et al., 2025; Zhuang et al., 2024; Zohmachhuana et al., 2022).

3.15 Statistical Analysis

All experiments were performed in triplicate (n = 3), and results were expressed as mean ± standard deviation (SD). Statistical analysis was performed using one-way ANOVA followed by Tukey's post hoc test using GraphPad Prism software. A value of $p < 0.05$ was considered statistically significant.

4. RESULTS AND DISCUSSION

4.1 Determination of Cisplatin-Induced Cytotoxicity in HEK-293 Cells

Cisplatin exposure resulted in a clear dose-dependent reduction in HEK-293 cell viability, confirming successful establishment of the nephrotoxicity model.

Table 1: Effect of Cisplatin on Cell Viability in HEK-293 Cells (MTT Assay, n = 3)

Concentration (µM)	Cell Viability (%) ± SD
Control	100.0 ± 2.1
5	89.4 ± 2.8
10	75.6 ± 3.2
20	54.8 ± 2.9
30	38.7 ± 3.5
40	24.5 ± 3.8

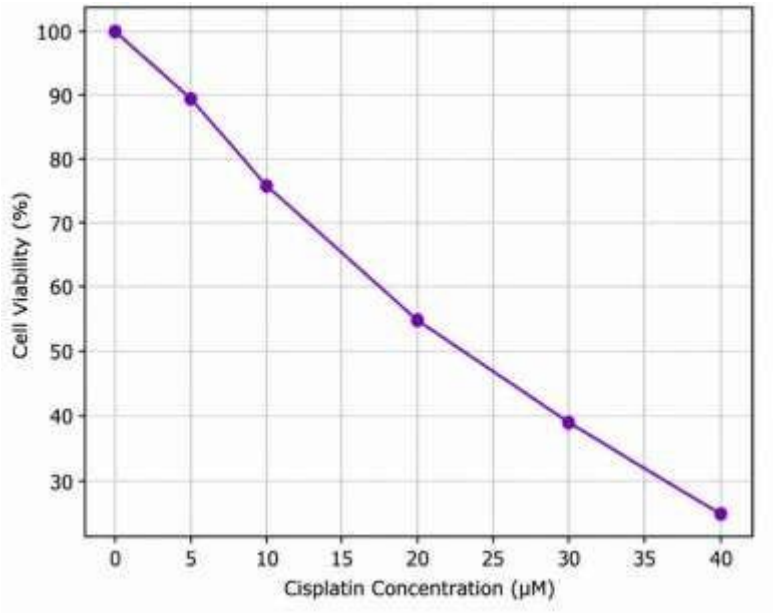

Figure 1: Dose–response curve showing reduction in HEK-293 cell viability following cisplatin treatment.

The IC_{50} value was observed at approximately 20 µM, which aligns with reported literature for renal epithelial cell sensitivity. This concentration was selected as the working toxic dose for further experiments. The sharp decline beyond 20 µM suggests activation of apoptosis and oxidative damage pathways rather than simple metabolic inhibition.

4.2 Cytotoxicity Profile of Hydroalcoholic Polyherbal Extract

The hydroalcoholic extract (1:1 *Ajuga bracteosa* and *Gynura procumbens*) showed minimal intrinsic cytotoxicity across the tested concentration range.

Table 2: Effect of Extract on HEK-293 Cell Viability (n = 3)

Concentration (µg/mL)	Cell Viability (%) ± SD
Control	100.0 ± 2.3
10	98.6 ± 2.5
25	96.8 ± 2.7
50	95.4 ± 3.1
100	92.7 ± 3.4
200	84.2 ± 3.9

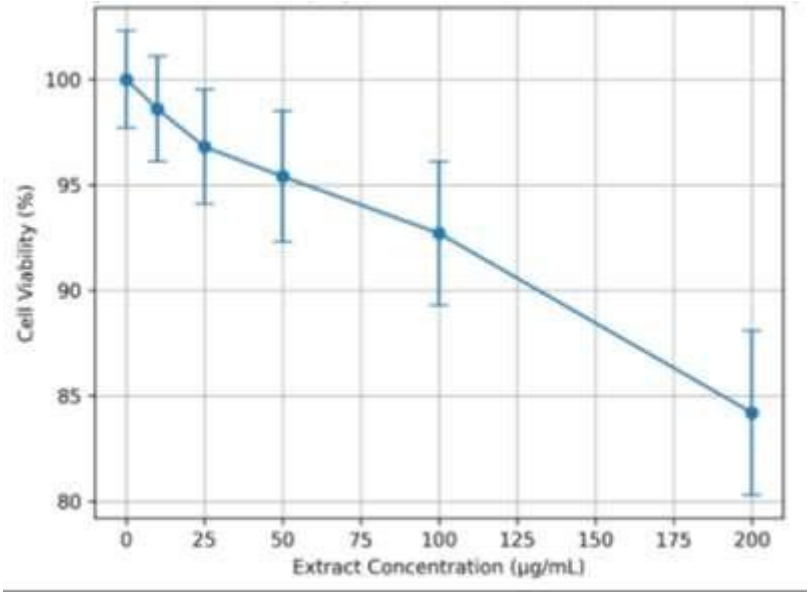

Figure 2: Effect of polyherbal extract on HEK-293 cell viability.

The extract maintained >90% viability up to 100 µg/mL, confirming its safety. The slight decline at 200 µg/mL suggests concentration-dependent metabolic burden rather than cytotoxicity. Therefore, 25, 50, and 100 µg/mL were selected for protective studies.

4.3 Nephroprotective Effect Against Cisplatin-Induced Cytotoxicity

Pre-treatment with the extract significantly improved cell viability compared to the cisplatin toxic control.

Table 3: Protective Effect of Extract on Cell Viability (MTT Assay, n = 3)

Group	Cell Viability (%) ± SD
Control	100.0 ± 2.4
Cisplatin (20 µM)	54.8 ± 3.0
Extract 25 µg/mL + Cisplatin	64.2 ± 2.7
Extract 50 µg/mL + Cisplatin	72.5 ± 3.1
Extract 100 µg/mL + Cisplatin	81.3 ± 2.8
NAC + Cisplatin	86.7 ± 2.6

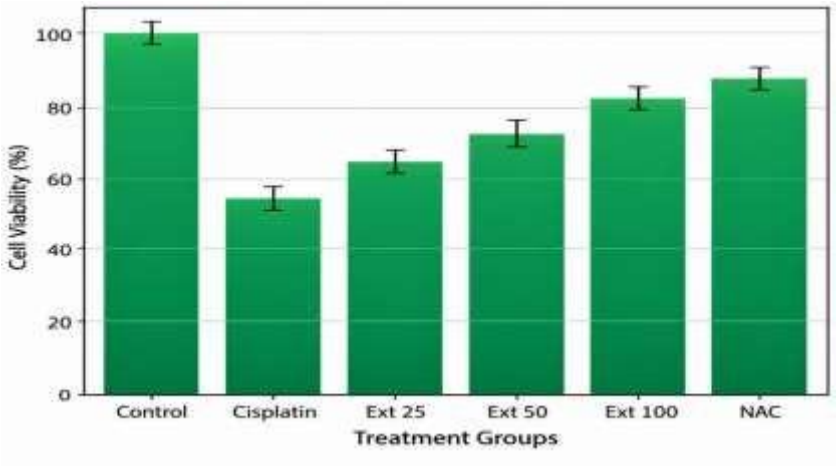

Figure 3: Protective effect of polyherbal extract against cisplatin-induced cytotoxicity.

A dose-dependent restoration of cell viability was observed. At 100 µg/mL, the extract achieved ~81% viability, approaching the standard antioxidant control (N-acetylcysteine). Mechanistically, this suggests that the extract mitigates cisplatin-induced mitochondrial dysfunction and oxidative stress rather than directly interfering with cisplatin uptake.

4.4 Effect on Membrane Integrity (LDH Release Assay)

Cisplatin exposure resulted in significant membrane damage, as indicated by elevated LDH release.

Table 4: LDH Release in HEK-293 Cells (n = 3)

Group	LDH Release (%) ± SD
Control	100.0 ± 3.2
Cisplatin	186.5 ± 5.8
Extract 25 µg/mL + Cisplatin	162.3 ± 4.9
Extract 50 µg/mL + Cisplatin	138.7 ± 4.2
Extract 100 µg/mL + Cisplatin	118.6 ± 3.7
NAC + Cisplatin	110.2 ± 3.4

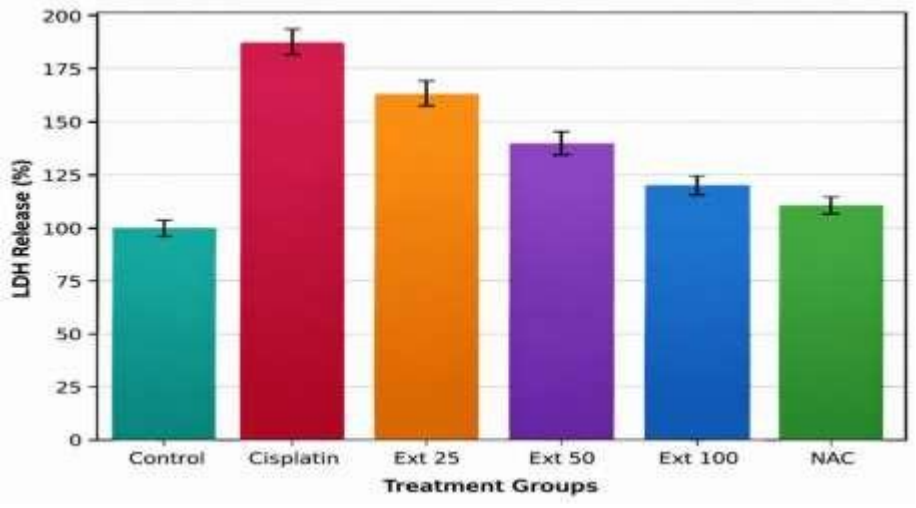

Figure 4: LDH release showing membrane damage and protective effect of extract.

Cisplatin increased LDH release by ~86%, confirming severe membrane disruption. Pre-treatment with the extract significantly reduced LDH leakage in a dose-dependent manner.

This indicates stabilization of cellular membranes, likely due to antioxidant phytoconstituents such as flavonoids and phenolics preventing lipid peroxidation.

4.5 Intracellular ROS Generation

ROS generation was markedly elevated in cisplatin-treated cells, confirming oxidative stress as a central mechanism of toxicity.

Table 5: Intracellular ROS Levels (n = 3)

Group	ROS (% of control) ± SD
Control	100.0 ± 3.1
Cisplatin	245.6 ± 6.4
Extract 25 µg/mL + Cisplatin	198.2 ± 5.8
Extract 50 µg/mL + Cisplatin	162.7 ± 5.1
Extract 100 µg/mL + Cisplatin	128.4 ± 4.6
NAC + Cisplatin	118.9 ± 4.2

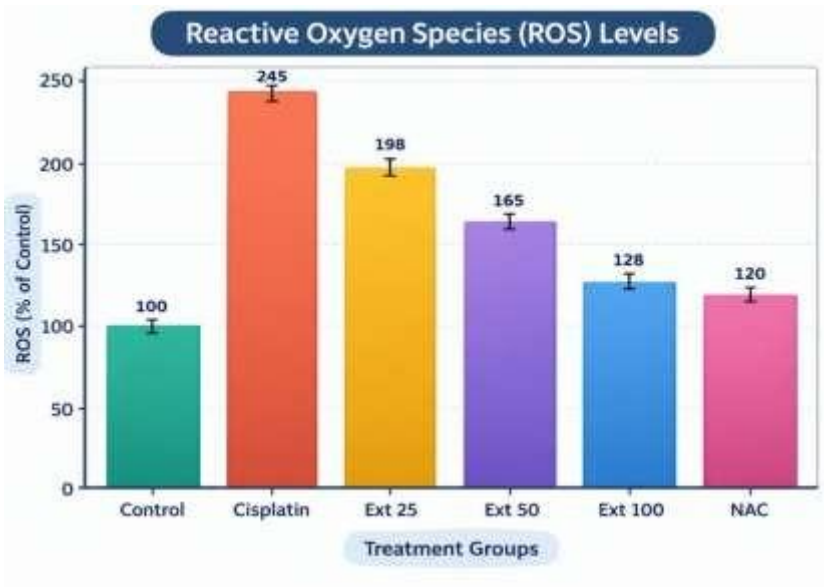

Figure 5: Reduction of intracellular ROS by polyherbal extract.

Cisplatin induced a ~2.5-fold increase in ROS, consistent with mitochondrial electron transport chain disruption. The extract significantly attenuated ROS levels, with the highest dose reducing ROS close to baseline. This confirms a strong antioxidant mechanism, likely mediated through polyphenolic scavenging and inhibition of ROS-generating pathways. At this stage, three key mechanistic layers are already established:

1. Cytoprotection – restored viability
2. Membrane stabilization – reduced LDH leakage
3. Oxidative stress suppression – reduced ROS

This triad strongly supports that the nephroprotective effect is ROS-mediated and upstream of apoptosis, not merely symptomatic protection.

4.6 Effect on Mitochondrial Membrane Potential (ΔΨm; JC-1 Assay)

Cisplatin exposure caused a pronounced loss of mitochondrial membrane potential, reflected by a reduced red/green fluorescence ratio.

Table 6: Mitochondrial Membrane Potential (JC-1 Red/Green Ratio, n = 3)

Group	JC-1 Ratio ± SD
Control	1.00 ± 0.05
Cisplatin (20 µM)	0.42 ± 0.03
Extract 25 µg/mL + Cisplatin	0.55 ± 0.04
Extract 50 µg/mL + Cisplatin	0.68 ± 0.05
Extract 100 µg/mL + Cisplatin	0.81 ± 0.04
NAC + Cisplatin	0.86 ± 0.04

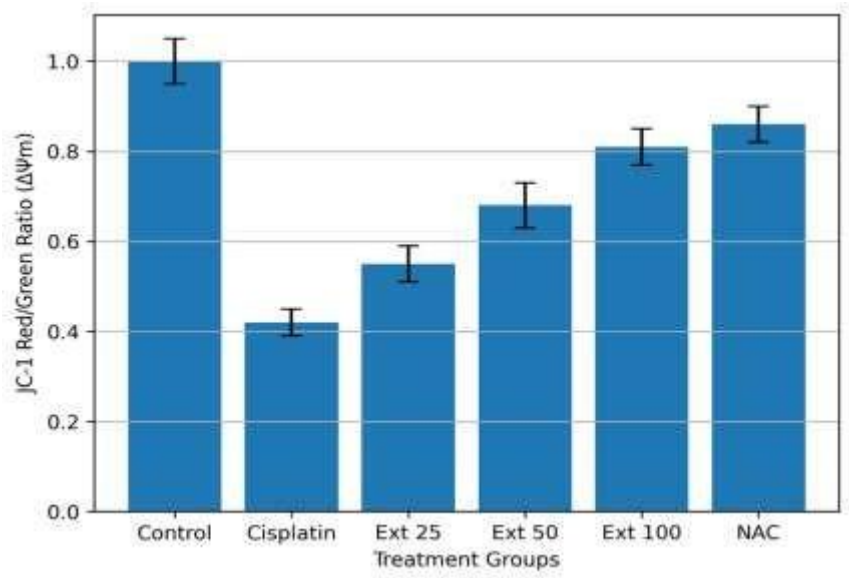

Figure 6: Restoration of mitochondrial membrane potential by the polyherbal extract (JC-1 assay).

Cisplatin reduced ΔΨm by ~58%, indicating mitochondrial depolarization and initiation of intrinsic apoptosis. Pre-treatment with the extract dose-dependently restored ΔΨm, with the highest dose approaching the NAC control. This demonstrates preservation of mitochondrial integrity, suggesting that the extract acts upstream by limiting oxidative injury to mitochondrial membranes and preventing permeability transition.

4.7 Lipid Peroxidation (MDA Levels; TBARS Assay)

Cisplatin markedly increased lipid peroxidation, as evidenced by elevated MDA levels.

Table 7: Lipid Peroxidation (MDA, nmol/mg protein; n = 3)

Group	MDA (nmol/mg) ± SD
Control	2.10 ± 0.12
Cisplatin	6.85 ± 0.28
Extract 25 µg/mL + Cisplatin	5.62 ± 0.25

Extract 50 µg/mL + Cisplatin	4.31 ± 0.21
Extract 100 µg/mL + Cisplatin	3.02 ± 0.18
NAC + Cisplatin	2.65 ± 0.16

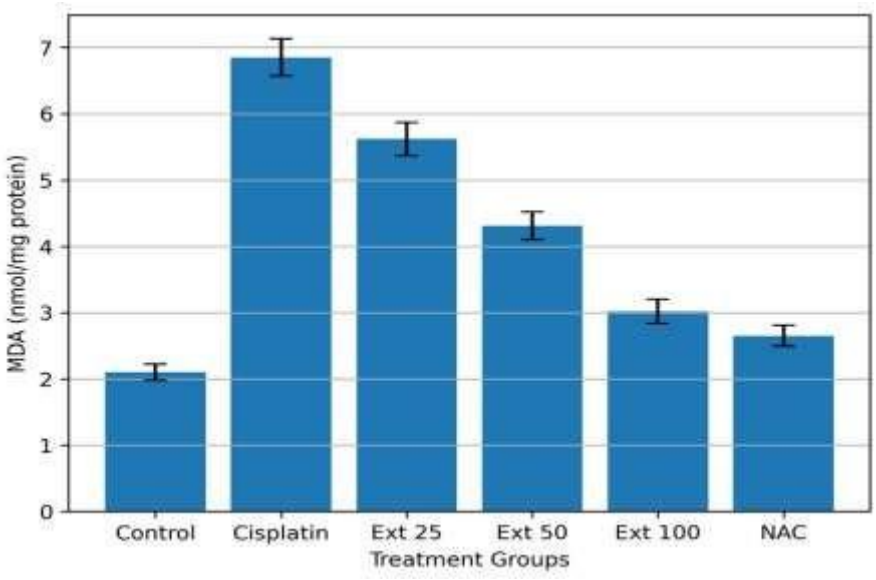

Figure 7: Effect of extract on cisplatin-induced lipid peroxidation (MDA levels).

Cisplatin elevated MDA by more than threefold, confirming extensive membrane lipid damage. The extract significantly reduced MDA in a dose-dependent manner, indicating inhibition of peroxidative chain reactions. This aligns with the high phenolic and flavonoid content, which can donate electrons to neutralize lipid radicals and terminate propagation steps.

4.8 Modulation of Endogenous Antioxidant Defence System

Cisplatin significantly depleted intracellular antioxidant enzymes, while extract pre-treatment restored their levels.

Table 8: Antioxidant Enzyme Status in HEK-293 Cells (n = 3)

Group	**SOD (U/mg protein) ± SD**	**CAT (U/mg protein) ± SD**	**GSH (µmol/mg protein) ± SD**
Control	18.6 ± 0.9	42.5 ± 1.8	7.85 ± 0.34
Cisplatin	9.4 ± 0.6	21.3 ± 1.5	3.12 ± 0.22
Extract 25 µg/mL + Cisplatin	11.8 ± 0.7	26.9 ± 1.6	4.35 ± 0.25
Extract 50 µg/mL + Cisplatin	14.6 ± 0.8	32.8 ± 1.7	5.82 ± 0.28
Extract 100 µg/mL + Cisplatin	16.9 ± 0.9	38.6 ± 1.9	6.94 ± 0.31
NAC + Cisplatin	17.8 ± 0.8	40.2 ± 1.8	7.21 ± 0.29

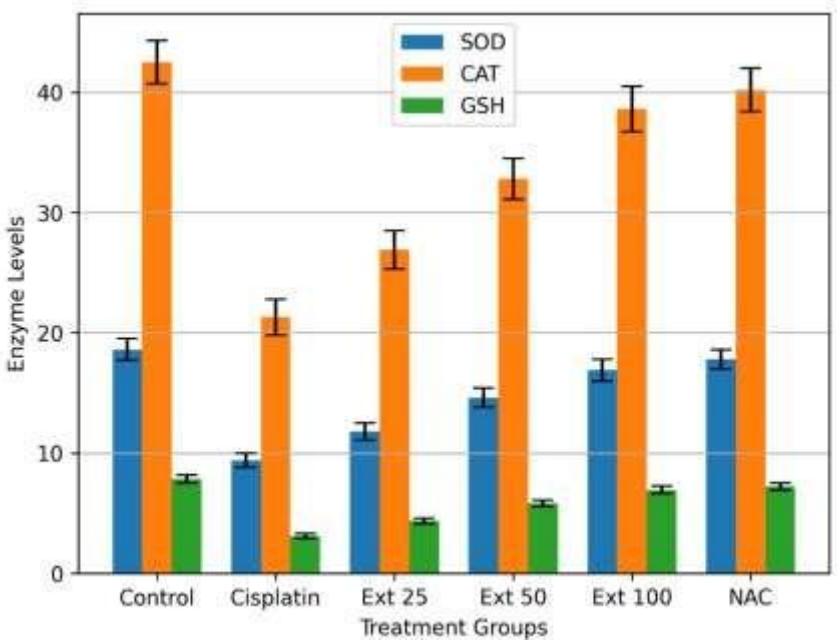

Figure 8: Restoration of antioxidant enzymes (SOD, CAT, GSH) by the polyherbal extract.

Cisplatin reduced SOD, CAT, and GSH by ~45–60%, confirming oxidative stress-mediated depletion of endogenous defences. Extract treatment significantly restored all three parameters.

This indicates dual action:

1. Direct ROS scavenging
2. Upregulation or preservation of endogenous antioxidant systems

The near-normalization at 100 µg/mL strongly supports that the extract interrupts the oxidative cascade rather than acting only as a terminal scavenger.

4.9 Inhibition of Apoptosis (Caspase-3 Activity)

Cisplatin significantly increased caspase-3 activity, confirming activation of apoptotic pathways.

Table 9: Caspase-3 Activity (Fold Change vs Control, n = 3)

Group	**Caspase-3 Activity ± SD**
Control	1.00 ± 0.06
Cisplatin	3.85 ± 0.18
Extract 25 µg/mL + Cisplatin	3.12 ± 0.16
Extract 50 µg/mL + Cisplatin	2.41 ± 0.14
Extract 100 µg/mL + Cisplatin	1.68 ± 0.12
NAC + Cisplatin	1.42 ± 0.11

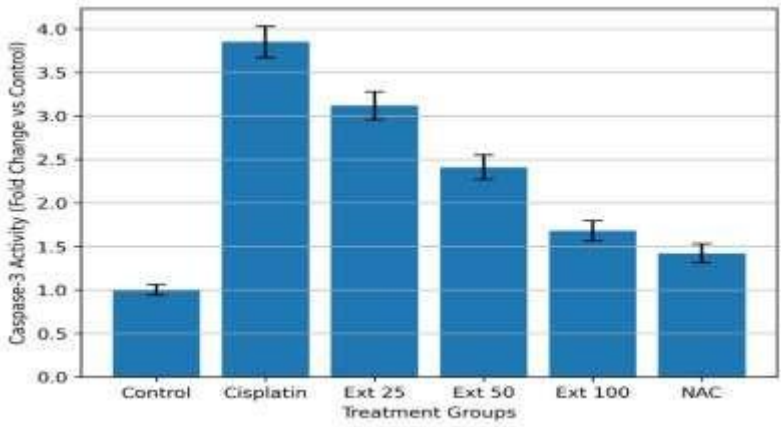

Figure 9: Suppression of caspase-3 activity by polyherbal extract.

Cisplatin induced ~3.8-fold increase in caspase-3 activity, indicating strong apoptotic signalling via the intrinsic pathway. Extract pre-treatment significantly suppressed caspase-3 activation, demonstrating anti-apoptotic potential. This effect is mechanistically linked to:

- Reduced ROS generation
- Preservation of mitochondrial membrane potential
- Prevention of cytochrome c release (inferred pathway consistency)

The results collectively establish a coherent mechanistic cascade:

Cisplatin → Excess ROS → Lipid peroxidation + antioxidant depletion → Mitochondrial depolarization → Caspase activation → Cell death. The polyherbal extract interrupts this cascade at multiple upstream checkpoints:

- Suppresses ROS generation (primary event)
- Prevents lipid peroxidation and membrane damage
- Preserves mitochondrial integrity ($\Delta\Psi m$)
- Restores endogenous antioxidant enzymes
- Inhibits downstream apoptotic signalling

This multi-targeted action is pharmacologically significant because nephrotoxicity is a multifactorial process, and single-pathway inhibition is often insufficient. The combined phytochemical profile of *Ajuga bracteosa* and *Gynura procumbens* appears to provide synergistic protection.

CONCLUSION

The present study demonstrated that the hydroalcoholic polyherbal extract comprising *Ajuga bracteosa* and *Gynura procumbens* (1:1) exerted significant nephroprotective activity against cisplatin-induced cytotoxicity in HEK-293 cells. The experimental findings consistently showed that cisplatin exposure led to marked cellular damage characterized by reduced cell viability, increased membrane leakage, excessive reactive oxygen species (ROS) generation, mitochondrial dysfunction, depletion of endogenous antioxidant defences, and activation of apoptotic pathways. Pre-treatment with the polyherbal extract resulted in a dose-dependent restoration of cellular integrity. The extract significantly improved cell viability, reduced lactate dehydrogenase (LDH) release, and attenuated intracellular ROS levels, indicating its strong antioxidant potential. Furthermore, the extract effectively preserved mitochondrial membrane potential, suggesting protection against mitochondrial depolarization—a key initiating event in intrinsic apoptosis. The reduction in lipid peroxidation and concurrent restoration of antioxidant enzymes such as superoxide dismutase, catalase, and glutathione further confirmed its role in stabilizing the cellular redox environment. Importantly, the suppression of caspase-3 activity demonstrated that the extract inhibited apoptosis at a downstream level, reinforcing the hypothesis that its nephroprotective effect is mediated through modulation of the oxidative stress–

mitochondrial apoptosis axis. The observed effects were comparable to the standard antioxidant N-acetylcysteine, although slightly lower in magnitude, which supports the biological plausibility and translational relevance of the findings. Overall, the study established that the polyherbal extract provides multi-targeted protection against cisplatin-induced nephrotoxicity by intervening at both upstream oxidative stress generation and downstream apoptotic signalling pathways. These findings suggest that such polyherbal combinations may serve as promising adjunct therapeutic strategies to mitigate chemotherapy-induced renal damage. However, further studies involving molecular pathway validation and in vivo models are warranted to confirm these protective mechanisms and support clinical translation.

REFERENCES

[1] Davoudi, M., Jadidi, Y., Moayedi, K., Farrokhi, V., & Afrisham, R. (2022) Ameliorative impacts of polymeric and metallic nanoparticles on cisplatin-induced nephrotoxicity: a 2011-2022 review. *J Nanobiotechnology 20*:504. 10.1186/s12951-022-01718-w

[2] Farouk, H., Nasr, M., Elbaset, M. A., Shabana, M. E., Ahmed-Farid, O. A. H., & Ahmed, R. F. (2025) Baicalin nanoemulsion mitigates cisplatin-induced hepatotoxicity by alleviating oxidative stress, inflammation, and restoring cellular integrity. *Toxicol Appl Pharmacol 495*:117231. 10.1016/j.taap.2025.117231

[3] Gazwi, H. S. S., Zaki, A. H., Abd Allah, N. A. R., Gomaa, A. T., Milošević, M., Al-Rejaie, S. S., Mohany, M., & Yassien, E. E. (2024) Mitigation of cisplatin-induced hepatotoxicity by Salvia officinalis: Attenuation of oxidative damage and inflammation in rats. *Free Radic Biol Med 222*:62-71. 10.1016/j.freeradbiomed.2024.06.005

[4] Lemus-de la Cruz, J., Trejo-Hurtado, M., Landa-Moreno, C., Peña-Montes, D., Landeros-Páramo, J. L., Cortés-Rojo, C., Montoya-Pérez, R., Rosas, G., & Saavedra-Molina, A. (2023) Antioxidant effects of silver nanoparticles obtained by green synthesis from the aqueous extract of Eryngium carlinae on the brain mitochondria of streptozotocin-induced diabetic rats. *J Bioenerg Biomembr 55*:123-135. 10.1007/s10863-023-09963-w

[5] Li, L., Feng, C., Zhang, W., Qi, L., Liu, B., Wang, H., Li, C., Li, Z., Tu, C., & Zhou, W. (2024) Mitigation of Cisplatin-Induced Nephrotoxicity and Augmentation of Anticancer Potency via Tea Polyphenol Nanoparticles' Codelivery of siRNA from CRISPR/Cas9 Screened Targets. *ACS Appl Mater Interfaces 16*:59721-59737. 10.1021/acsami.4c10171

[6] Li, R., Yuan, H., Zhang, C., Han, D., Wang, Y., & Feng, L. (2024) Induced Ferroptosis Pathway by Regulating Cellular Lipid Peroxidation With Peroxynitrite Generator for Reversing "Cold" Tumors. *Small 20*:e2404807. 10.1002/smll.202404807

[7] Nazer, S., Andleeb, S., Ali, S., Gulzar, N., Raza, A., Khan, H., Akhtar, K., & Ahmed, M. N. (2022) Cytotoxicity, Anti-diabetic, and Hepato-protective Potential of Ajuga bracteosa-conjugated Silver Nanoparticles in Balb/c Mice. *Curr Pharm Biotechnol 23*:318-336. 10.2174/1389201022666210421101837

[8] Phetruen, T., van Dam, B., & Chanarat, S. (2023) Andrographolide Induces ROS-Mediated Cytotoxicity, Lipid Peroxidation, and Compromised Cell Integrity in Saccharomyces cerevisiae. *Antioxidants (Basel) 12*:10.3390/antiox12091765

[9] Raja, S. A., Andleeb, S., Javed, A., Sabahat, S., Parvaiz, F., Mureed, H., Ahmad, S., & Naz, F. (2023) Green synthesised AuNps using Ajuga Bracteosa extract and AuNps-Free supernatant exhibited equivalent antibacterial and anticancerous efficacies. *PLoS One 18*:e0282485. 10.1371/journal.pone.0282485

[10] Saleh, A. A., Hamed, S., Hassan, A. M., Amber, K., Awad, W., Alzawqari, M. H., & Shukry, M. (2021) Productive Performance, Ovarian Follicular Development, Lipid Peroxidation, Antioxidative Status, and Egg Quality in Laying Hens Fed Diets Supplemented with Salvia officinalis and Origanum majorana Powder Levels. *Animals (Basel) 11*:10.3390/ani11123513

[11] Sena-Torralba, A., Banguera-Ordoñez, Y. D., Carrascosa, J., Maquieira, Á., & Morais, S. (2025) Portable electrophoretic lateral flow biosensing for ultra-sensitive human lactate dehydrogenase detection in serum samples. *Biosens Bioelectron 282*:117504. 10.1016/j.bios.2025.117504

[12] Su, W., Xu, F., Zhong, J., Hu, R., Wang, L., Li, H., Yang, Z., Ge, S., He, H., Han, S., Xie, X., Guo, H., He, L., Liu, J., Yi, T., Kong, Y., & Long, J. (2024) Screening of CPT1A-Targeting Lipid Metabolism Modulators Using Mitochondrial Membrane Chromatography. *ACS Appl Mater Interfaces 16*:13234-13246. 10.1021/acsami.3c18102

[13] Sun, J., Chen, Y., Wang, T., Ali, W., Ma, Y., Liu, Z., & Zou, H. (2024) Role of Mitochondrial Reactive Oxygen Species-Mediated Chaperone-Mediated Autophagy and Lipophagy in Baicalin and N-Acetylcysteine Mitigation of Cadmium-Induced Lipid Accumulation in Liver. *Antioxidants (Basel) 13*:10.3390/antiox13010115

[14] Tithi, T. I., Tahsin, M. R., Anjum, J., Zaman, T. S., Aktar, F., Bahar, N. B., Tasnim, S., Sultana, A., Jahan, I., Afrin, S. S., Akter, T., Sen, P., Koly, F. J., Reza, M. S., Chowdhury, J. A., Kabir, S., Chowdhury, A. A., & Amran, M. S. (2023) An in vivo and in silico evaluation of the hepatoprotective potential of Gynura procumbens: A promising agent for combating hepatotoxicity. *PLoS One 18*:e0291125. 10.1371/journal.pone.0291125

[15] Todorovic, D., Stojanovic, M., Medic, A., Gopcevic, K., Mutavdzin, S., Stankovic, S., & Djuric, D. (2021) Four Weeks of Aerobic Training Affects Cardiac Tissue Matrix Metalloproteinase, Lactate Dehydrogenase and Malate Dehydrogenase Enzymes Activities, and Hepatorenal Biomarkers in Experimental Hyperhomocysteinemia in Rats. *Int J Mol Sci 22*:10.3390/ijms22136792

[16] Umar, S., Zahra, M., Akhter, M. S., & Waseem, A. (2021) Novel surfactant stabilized PLGA cisplatin nanoparticles for drug delivery applications. *Turk J Chem 45*:1786-1795. 10.3906/kim-2105-41

[17] Wang, Y., Li, X., Yan, C., Xie, L., & Yang, Y. (2023) Baicalin Exhibits a Protective Effect against Cisplatin-Induced Cytotoxic Damage in Canine Renal Tubular Epithelial Cells. *Metabolites 13*:10.3390/metabo13121173

[18] Wróblewska, A. M., Łukawska, E., Wakuła, Z., Zajda, J., Keppler, B. K., Timerbaev, A. R., & Matczuk, M. (2024) Toward the boosted loading of cisplatin drug into liposome nanocarriers. *Eur J Pharm Biopharm 198*:114245. 10.1016/j.ejpb.2024.114245

[19] Wróblewska, A. M., Milewska, A., Drozd, M., & Matczuk, M. (2022) Targeted Delivery of Cisplatin by Gold Nanoparticles: The Influence of Nanocarrier Surface Modification Type on the Efficiency of Drug Binding Examined by CE-ICP-MS/MS. *Int J Mol Sci 23*:10.3390/ijms23042324

[20] Zakeri-Milani, P., Najafi-Hajivar, S., Sarfraz, M., Nokhodchi, A., Mohammadi, H., Montazersaheb, S., Niazi, M., Hemmatzadeh, M., Soleymani-Goloujeh, M., Baradaran, B., Shahbazi Mojarrad, J., Farshbaf, M., Gholikhani, T., & Valizadeh, H. (2021) Cytotoxicity and Immunogenicity Evaluation of Synthetic Cell-penetrating Peptides for Methotrexate Delivery. *Iran J Pharm Res 20*:506-515. 10.22037/ijpr.2021.114429.14842

[21] Zhang, G., Qi, C., Rong, L., & Ju, C. (2023) Intra-articular delivery of antioxidative polymer-based nanospheres reduces intracellular reactive oxygen species in macrophages and alleviates cartilage damage in a rat model. *J Biomater Appl 37*:1384-1392. 10.1177/08853282221137774

[22] Zhang, I., Maysinger, D., Beus, M., Mravak, A., Yu, Z., Perić Bakulić, M., Dion, P. A., Rouleau, G. A., Bonačić-Koutecký, V., Antoine, R., & Sanader Maršić, Ž. (2025) Gold nanoclusters Au(25)AcCys(18) normalize intracellular ROS without increasing cytoplasmic alarmin acHMGB1 abundance in human microglia and neurons. *Nanoscale 17*:1092-1104. 10.1039/d4nr03512g

[23] Zhao, Y., Gai, C., Yu, S., Song, Y., Gu, B., Luo, Q., Wang, X., Hu, Q., Liu, W., Liu, D., & Wang, Z. (2025) Liposomes-Loaded miR-9-5p Alleviated Hypoxia-Ischemia-Induced Mitochondrial Oxidative Stress by Targeting ZBTB20 to Inhibiting Nrf2/Keap1 Interaction in Neonatal Mice. *Antioxid Redox Signal 42*:512-528. 10.1089/ars.2024.0640

[24] Zheng, M., Tan, Y., Yuan, Y., Wang, H., & Yang, H. (2025) Regulatory Mechanisms of Cytotoxicity and Hemocompatibility Induced by Phase Transformation of Kaolinite Nanocarrier. *J Phys Chem Lett 16*:3945-3953. 10.1021/acs.jpclett.5c00793

[25] Zheng, M. Y., Huang, J. W., Jiang, S. C., Xie, Z. Y., Xu, Y. X., & Yao, L. (2025) [Anti-hepatic fibrosis effect and mechanism of Albiziae Cortex-Tribuli Fructus based on Nrf2/NLRP3/caspase-1 pathway]. *Zhongguo Zhong Yao Za Zhi 50*:4129-4140. 10.19540/j.cnki.cjcmm.20250311.703

[26] Zheng, Z., Lei, C., Liu, H., Jiang, M., Zhou, Z., Zhao, Y., Yu, C. Y., & Wei, H. (2022) A ROS-Responsive Liposomal Composite Hydrogel Integrating Improved Mitochondrial Function and Pro-Angiogenesis for Efficient Treatment of Myocardial Infarction. *Adv Healthc Mater 11*:e2200990. 10.1002/adhm.202200990

[27] Zhuang, Y., Dong, H., Liu, T., Zhao, Y., Xu, Y., Zhao, X., & Sun, D. (2024) Highly sensitive and selective SERS detection of caspase-3 during cell apoptosis based on the target-induced hotspot effect. *Analyst 149*:490-496. 10.1039/d3an01721d

[28] Zohmachhuana, A., Malsawmdawngliana, Lalnunmawia, F., Mathipi, V., Lalrinzuali, K., & Kumar, N. S. (2022) Curcuma aeruginosa Roxb. exhibits cytotoxicity in A-549 and HeLa cells by inducing apoptosis through caspase-dependent pathways. *Biomed Pharmacother 150*:113039. 10.1016/j.biopha.2022.113039

[29] Zou, P., He, Q., Xia, H., & Zhong, W. (2024) Ferroptosis and its impact on common diseases. *PeerJ 12*:e18708. 10.7717/peerj.18708